UCRL -8982

UNIVERSITY OF CALIFORNIA

Ernest O. Lawrence Radiation Laboratory

TWO-WEEK LOAN COPY

This is a Library Circulating Copy
which may be borrowed for two weeks.
For a personal retention copy, call
Tech. Info. Division, Ext. 5545

BERKELEY, CALIFORNIA

DISCLAIMER

This document was prepared as an account of work sponsored by the United States Government. While this document is believed to contain correct information, neither the United States Government nor any agency thereof, nor the Regents of the University of California, nor any of their employees, makes any warranty, express or implied, or assumes any legal responsibility for the accuracy, completeness, or usefulness of any information, apparatus, product, or process disclosed, or represents that its use would not infringe privately owned rights. Reference herein to any specific commercial product, process, or service by its trade name, trademark, manufacturer, or otherwise, does not necessarily constitute or imply its endorsement, recommendation, or favoring by the United States Government or any agency thereof, or the Regents of the University of California. The views and opinions of authors expressed herein do not necessarily state or reflect those of the United States Government or any agency thereof or the Regents of the University of California.

UCRL-8982

UNIVERSITY OF CALIFORNIA

Lawrence Radiation Laboratory
Berkeley, California

Contract No. W-7405-eng-48

DIRECT NUCLEON-NUCLEON COLLISIONS INSIDE THE NUCLEUS ACCORDING TO THE IMPULSE APPROXIMATION

Thomas P. Clements and Lester Winsberg

August 11, 1960

DIRECT NUCLEON-NUCLEON COLLISIONS INSIDE THE NUCLEUS ACCORDING TO THE IMPULSE APPROXIMATION

Thomas P. Clements and Lester Winsberg

Lawrence Radiation Laboratory
Universiety of California
Berkeley, California

August 11, 1960

ABSTRACT

Direct nucleon-nucleon collisions play an important role in high-energy nuclear reactions. The importance of such collisions at lower energies is not clear. To aid in the interpretation of nuclear reactions, we have analyzed the collisions between an incident nucleon and nucleons in a Fermi gas by means of the impulse approximation. The treatment given here is based on information from nucleon-nucleon scattering experiments. Collisions inside a nucleus are considered to be the same as those in the unbound state at the same center-of-mass energy, except for the effect of the Pauli exclusion principle. The effective elastic and inelastic cross section, $\langle\sigma\rangle$, between like and unlike nucleons is computed for incident energies from 10 Mev to 6 Bev at several values of the Fermi energy. The properties of the struck nucleons in allowed collisions are also calculated. This information may prove useful in interpreting some recoil experiments. Analytical expressions for $\langle\sigma\rangle$ and quantities related to the struck nucleon are given for elastic collisions in which the scattering is isotropic and the free-particle cross sections are either constant or vary inversely as the bombarding energy.

DIRECT NUCLEON-NUCLEON COLLISIONS INSIDE THE NUCLEUS ACCORDING TO THE IMPULSE APPROXIMATION

Thomas P. Clements and Lester Winsberg

Lawrence Radiation Laboratory
University of California
Berkeley, California

August 11, 1960

INTRODUCTION

The processes that occur during a nuclear reaction are not well known. One usually assumes that the collision between a high-energy particle and a nucleon inside a nucleus is essentially the same as in the unbound state at the same center-of-mass energy, except for the effect of the Pauli exclusion principle. In line with this "impulse approximation", information obtained from p-p, n-p, and π-p scattering experiments has been used in the analysis of nuclear reactions induced by high-energy particles.[1] This type of analysis has been successful in interpreting the available information on reactions induced by particles with energies of 1 Bev or less. However, serious discrepancies appear at higher energies.[1,2]

An analysis of nuclear reactions by means of the impulse approximation would be facilitated if the values of the effective collision cross sections $\langle\sigma\rangle$ of neutrons and protons inside nuclear matter were known at all energies. This information would be especially helpful for a study of the simpler reactions in which one or at most a few nucleons are emitted. The distance the incident particle penetrates the nucleus and the probability of escape of the collision products could be directly calculated from the values of $\langle\sigma\rangle$. The experimentally determined values of the cross sections, angular distributions,

and kinetic energies of the products of the simpler nuclear reactions could then be compared with the results of a "one-step" calculation. In the calculation of Metropolis et al., these reactions are treated along with all the other reactions that occur.[1]

The values of $\langle \sigma \rangle$ have been previously estimated over a restricted range of incident energies, usually limited to cases in which the scattering is isotropic in the center-of-mass system.[3-9] The analytical solution of the general case is very complex. For this reason we have computed $\langle \sigma \rangle$ on the IBM-701 computer, by means of the Monte Carlo method, for incident energies from 10 Mev to 6 Bev at several values of the Fermi energy. The nucleus is assumed to consist of neutron and proton Fermi gases. Collisions between two protons and between two neutrons are considered to be equivalent. In addition, we have calculated various quantities related to the momentum of the struck nucleons in allowed collisions. This information should prove useful in interpreting some recoil experiments.

CALCULATION

In Part A of this section we touch briefly on the kinematics of nucleon-nucleon collisions. In Part B we present analytical solutions for $\langle\sigma\rangle$ and the quantities related to the momentum of the struck nucleons for elastic collisions in which the scattering is isotropic in the center-of-mass system, and the free-particle cross section either remains constant or varies inversely with energy. The latter type of cross-section dependence occurs below 150 Mev for both p-p and n-p collisions. Above this energy the elastic p-p cross section is nearly constant until about 1 Bev. In Part C we consider the inelastic collisions. Part D of this section describes the machine computation.

A. Kinematics of Nucleon-Nucleon Collisions[10]

The collision between two moving nucleons in the laboratory system is shown in Fig. 1a. The momentum vectors are denoted by $\vec{p}$. The subscripts 1 and 2 refer to the incident and struck particles respectively. The collision angle, ω, is the angle between $\vec{p}_1$ and $\vec{p}_2$. The direction of motion of the center of mass is $\overrightarrow{CD}$, where C is the midpoint of AB. The initial trajectory of the two nucleons in the center-of-mass system lies along AB; the momentum of the incident particle in this system is given by $\overrightarrow{AC}$ and that of the struck particle by $\overrightarrow{BC}$, as shown in Figs. 1a and 1b. Quantities in the center-of-mass system are denoted by primed symbols: $\vec{p}'$ is the momentum vector; θ' is the scattering angle; and ϕ' is the azimuthal angle, i.e., the angle between the planes ACBD and AFBE. The angles α' and χ' will be of interest in the discussion of inelastic collisions (Part C below). After the collision, the incident particle is moving in the direction $\overrightarrow{CF}$ and the struck particle in the direction $\overrightarrow{CE}$, in the center-of-mass system. An inverse

Lorentz transformation gives the final energies of the nucleons in the laboratory system. The schematic representation of the transformation as given in Fig. 1 becomes distorted at relativistic energies.

For elastic collisions between particles of the same rest mass, m_0, the final energy of each particle is given by

$$E_{final} = \frac{E_1+E_2}{2} \pm \frac{E_1-E_2}{2} \cos\theta' \pm \frac{p_1 p_2}{\sqrt{2(A+1)}} \sin\omega \sin\theta' \cos\phi', \qquad (1)$$

where E_1 and E_2 are the energies of the incident and struck particles respectively and $A = \gamma_1\gamma_2 - p_1 p_2 \cos\omega$. The incident energy, E_1, is defined here as the energy of the incident particle inside the nucleus, i.e. the sum of its energy outside the nucleus and the energy of the potential well. For our purposes it is unnecessary to specify either of the latter two quantities, merely their sum. In this paper velocities, denoted by β, are in units of c, the velocity of light; momenta, p, are given in units of $m_0 c$, and the kinetic energies, E, in units of $m_0 c^2$, where m_0 is the free nucleon mass. The total energy of a particle in these units is $\gamma = 1+E$. The + sign of the second and third terms in Eq. (1) is for the incident particle, and the - sign is for the struck particle. Similar equations for the inelastic case will be given below.

The effective nucleon-nucleon collision cross section inside nuclear matter is given by

$$\langle\sigma\rangle = \frac{1}{2}\iiint \frac{\beta''}{\beta_1} P(p_2)\, dp_2\, d\cos\omega\, \frac{d\sigma}{d\Omega}(E'', \theta')\, d\Omega, \qquad (2)$$

where β'' and E'' are the velocity and kinetic energy respectively of the incident particle in the coordinate system of the struck particle, $P(p_2)dp_2$ is

the distribution in magnitude of the momenta of the struck particles, $d\sigma/d\Omega$ is the differential cross section, and E'' equals $A - 1$. The normalization factor 1/2 arises from the integration with respect to $\cos\omega$ between +1 and - 1. The other limits of integration are set by the requirement that the energy of each product of the collision be greater than the Fermi energy, E_F. For this purpose we set E_{final} equal to E_F in Eq. (1) and in equivalent expressions for inelastic collisions.

The average value of any variable x in permitted collisions is

$$\langle x \rangle = \frac{\langle \sigma x \rangle}{\langle \sigma \rangle} , \tag{3}$$

where $\langle \sigma x \rangle$ is obtained from Eq. (2) (or Eq. (4) below) by putting x under the integral sign.

B. Analytical Expressions for Isotropic Elastic Scattering

For isotropic elastic scattering, Eq. (2) reduces to

$$\langle \sigma \rangle = \frac{p_1}{2} \frac{\gamma_1}{\gamma_1+1} \int^{p_F} (1-2F+E_2/E_1)P(p_2)\,dp_2 \int_{-1}^{1} \frac{A+1}{A} \frac{\sigma\, d\cos\omega}{\left(p_1^2+p_2^2+2p_1p_2\cos\omega\right)^{1/2}}, \tag{4}$$

where we have $F = E_F/E_1$ and σ, the total free-particle scattering cross section, is a function of E''. The lower limit of the first integral sign is zero for $E_1 \geqslant 2E_F$. For $E_1 < 2E_F$, we have $E_2 = 2E_F - E_1$. In either case the upper limit is p_F, the Fermi momentum. For a Fermi gas, we have

$$P(p_2)dp_2 = 3p_2^2\, dp_2/p_F^3 . \tag{5}$$

The quantities $\langle\sigma\rangle$ and $\langle x\rangle$ can be expressed as power series in F. For relativistic energies, F is small and only the first term is significant. For nonrelativistic energies we obtain solutions to terms in F^2.

The integration of Eq. (4) with respect to $\cos\omega$ can be made exactly both for $\langle\sigma\rangle$ and $\langle\sigma x\rangle$ with the functions σ and with most of the variables x that we will consider. For $\langle\sigma\rangle$ when σ is constant, we have

$$\frac{p_1}{2}\int_{-1}^{1}\frac{A+1}{A}\frac{d\cos\omega}{\left(p_1^2+p_2^2+2p_1p_2\cos\omega\right)^{1/2}} = 1+\frac{1}{p_2\sqrt{a}}\tanh^{-1}\frac{p_2\sqrt{a}}{p_2^2+\gamma_1\gamma_2} \qquad (6)$$

where $a = (\gamma_1+\gamma_2)^2-1$. A similar expression has been derived for σ varying inversely with the energy.[5] The expressions for $\langle\sigma x\rangle$ are similar in form to Eq. (6) but involve more terms. For convenience we can alternatively make the expansion,

$$\begin{aligned}\frac{\gamma_1}{\gamma_1+1}\frac{A+1}{A}\frac{p_1}{\left(p_1^2+p_2^2+2p_1p_2\cos\omega\right)^{1/2}} = 1 &- \frac{\gamma_1}{2}\frac{p_2^2}{p_1^2} - \frac{1}{\gamma_1}\frac{p_2}{p_1}\cos\omega \\ &+ \frac{2\gamma_1^3-\gamma_1^2+2}{2\gamma_1^2}\frac{p_2^2}{p_1^2}\cos^2\omega \\ &- \frac{2\gamma_1^3-3\gamma_1^2-3\gamma_1+1}{2\gamma_1}\frac{p_2^3}{p_1^3}\cos\omega \\ &+ \frac{2\gamma_1^5-4\gamma_1^4-4\gamma_1^3+3\gamma_1^2-2}{\gamma_1^3}\frac{p_2^3}{p_1^3}\cos^3\omega \\ &+ \ldots\ldots, \qquad (7)\end{aligned}$$

and then integrate with respect to $\cos\omega$. For the nonrelativistic cases we set $\frac{\gamma_1}{\gamma_1+1} \cdot \frac{A+1}{A}$ equal to 1 and expand Eq. (7) to the fourth power in $\cos\omega$ and p_2/p_1. The first six terms of this expansion can be obtained from the right side of Eq. (7) by setting $\gamma_1 = 1$.

We also solve Eqs. (3) and (4) when σ varies inversely as E'', i.e., for

$$\sigma = \sigma_0 \, E_1/(A-1), \tag{8}$$

where σ_0 is the free-particle cross section at the incident energy E_1 with the struck particle at rest. Expressions similar to Eqs. (6) and (7) can be obtained for this case.

The solutions of Eqs. (3) and (4) for the lower limit of the first integral sign (integration with respect to p_2) equal to zero are given in Tables I to IV. We do not give any expressions for the condition $E_1 < 2E_F$, because the impulse approximation implicit in this entire treatment is not valid at low energies. However, they can be derived from Eq. (4) by setting the lower limit of the first integral equal to $(4E_F - 2E_1)^{1/2}$.[5,6] In addition to $\langle\sigma\rangle$, for allowed collisions we list $\langle p_2\rangle$, the average value of the momentum, p_2, of the struck particle; $\langle\cos\omega\rangle$, the average value of the cosine of the collision angle (see Fig. 1); $\langle p_2\cos\omega\rangle_{\cos\omega>0}$ and $\langle p_2\cos\omega\rangle_{\cos\omega<0}$, the average value of the projection of p_2 on the beam direction, $\overrightarrow{AD}$ (see Fig. 1) for positive and negative values of $\cos\omega$, respectively; and $\langle p_2\sin\omega\rangle$, the average absolute value of the projection of p_2 on the plane perpendicular to the beam direction.

In the INTRODUCTION and SUMMARY we consider the significance of these quantities for experimental studies of nuclear reactions. The expression for $\langle\sigma\rangle$ in Eq. (a) of Table I was originally derived by Goldberger.[3] For $E_1 < 2E_F$, other authors obtained[5,6]

$$\langle\sigma\rangle = \sigma_0 \left[1 - \frac{7}{5} F + \frac{2}{5} (2 - \frac{1}{F})^{5/2} F \right] \tag{9}$$

where $\sigma = \sigma_0$. The derivation of $\langle\sigma\rangle$ is also given for the case where σ varies as [5] $1/E$ or as [6] $1/(E+ \text{constant})$.

The solutions of Eqs. (3) and (4) given here are for like-particle scattering or for the unlike-particle case where the Fermi energy of the proton is identical to that of the neutron. Equations (2) to (4) can also be solved for different values of the Fermi energy. We denote E_F/E_1 for the proton by F_p and for the neutron by F_n. Here, we have

$$\langle\sigma\rangle = \frac{1}{2}\left(\langle\sigma\rangle_{F=F_p} + \sigma_{F=F_n} \right), \tag{10}$$

where $\langle\sigma\rangle_{F=F_p}$ and $\langle\sigma\rangle_{F=F_n}$ are the solutions of Eqs. (2) or (4). The limit, p_F, for both is that of the struck particle. The quantities $\langle x\rangle$ can be obtained in a similar fashion for this case. For $F_p \approx F_n$, Eq. (10) gives a result nearly the same as that from Eqs. (2) or (4).

In this section we have derived expressions for elastic isotropic scattering. The analytical solution of Eq. (2) for nonisotropic scattering is difficult because of the complexity of the experimental data.[11] It is, therefore, not presented here. Furthermore, the expressions given in Tables I to IV will be sufficient for the discussion given later.

A machine computation was performed for the solution of the general case. (See section D below)

Table I

Nonrelativistic expressions of $\langle\sigma\rangle$ and other quantities for isotropic scattering where $\sigma = \sigma_0$ and $E_1 \geqslant 2\,E_F$

a. $\langle\sigma\rangle$	$= \sigma_0 \left(1 - \frac{7}{5} F\right)$
b. $\langle p_2\rangle$	$= 3\, p_F\, \sigma_0 \left(1 - \frac{4}{3} F\right)/4 \langle\sigma\rangle$
c. $\langle\cos\omega\rangle$	$= - p_F\, \sigma_0 \left(1 - \frac{4}{3} F\right)/4 p_1 \langle\sigma\rangle = - \langle p_2\rangle / 3\, p_1$
d. $\langle p_2 \cos\omega\rangle_{\cos\omega > 0}$	$= 3\, p_F\, \sigma_0 \left(1 - \frac{8}{15} F^{1/2} - \frac{7}{6} F + \frac{24}{35} F^{3/2} - \frac{11}{48} F^2\right)/16 \langle\sigma\rangle$
e. $\langle p_2 \cos\omega\rangle_{\cos\omega < 0}$	$= - 3\, p_F \sigma_0 \left(1 + \frac{8}{15} F^{1/2} - \frac{7}{6} F - \frac{24}{35} F^{3/2} - \frac{11}{48} F^2\right)/16 \langle\sigma\rangle$
f. $\langle p_2 \cos\omega\rangle$	$= \langle p_2 \cos\omega\rangle_{\cos\omega > 0} + \langle p_2 \cos\omega\rangle_{\cos\omega < 0}$
g. $\langle p_2 \sin\omega\rangle$	$= 3\pi\, p_F \sigma_0 \left(1 - \frac{17}{12} F + \frac{37}{384} F^2\right)/16 \langle\sigma\rangle$

Table II

Relativistic expressions of $\langle\sigma\rangle$ and other quantities for isotropic scattering where $\sigma = \sigma_0$ and $E_1 \gg 2\,E_F$

a. $$\langle\sigma\rangle = \sigma_0\left(1 - \frac{7}{5}F - \frac{\gamma_1^3 + \gamma_1^2 - 2}{5\gamma_1^2(\gamma_1 + 1)}F\right)$$

b. $$\langle p_2\rangle = 3\,p_F\,\sigma_0\left(1 - \frac{4}{3}F - \frac{2(\gamma_1^3 + \gamma_1^2 - 2)}{9\gamma_1^2(\gamma_1 + 1)}F\right)/4\langle\sigma\rangle$$

c. $$\langle\cos\omega\rangle = -\,p_F\,\sigma_0\left(1 - \frac{4}{3}F + \frac{2(4\gamma_1^5 - 3\gamma_1^4 - 3\gamma_1^3 - 4\gamma_1^2 + 6)}{15\gamma_1^2(\gamma_1 + 1)}F\right)/4\gamma_1 p_1\langle\sigma\rangle$$

d. $$\langle p_2\cos\omega\rangle_{\cos\omega > 0} = 3p_F\sigma_0\left(1 - \frac{8}{15\gamma_1}\sqrt{\frac{2}{\gamma_1 + 1}}\,F^{1/2} - \frac{1}{3}\left\{4 + \frac{\gamma_1^2 - 2}{\gamma_1^2(\gamma_1 + 1)}\right\}F\right)/16\langle\sigma\rangle$$

e. $$\langle p_2\cos\omega\rangle_{\cos\omega < 0} = -\,3p_F\sigma_0\left(1 + \frac{8}{15}\gamma_1\sqrt{\frac{2}{\gamma_1 + 1}}\,F^{1/2} - \frac{1}{3}\left\{4 + \frac{\gamma_1^2 - 2}{\gamma_1^2(\gamma_1 + 1)}\right\}F\right)/16\langle\sigma\rangle$$

f. $$\langle p_2\cos\omega\rangle = \langle p_2\cos\omega\rangle_{\cos\omega > 0} + \langle p_2\cos\omega\rangle_{\cos\omega < 0}$$

g. $$\langle p_2\sin\omega\rangle = 3\pi\,p_F\sigma_0\left(1 - \frac{1}{3}\left\{4 + \frac{2\gamma_1^3 + \gamma_1^2 - 2}{2\gamma_1^2(\gamma_1 + 1)}\right\}F\right)/16\langle\sigma\rangle$$

Table III

Nonrelativistic expressions of $\langle\sigma\rangle$ and other quantities for isotropic scattering where σ is proportional to $1/E$ and $E_1 \geqslant 2\,E_F$

a. $\langle\sigma\rangle = \sigma_0\,(1 - \frac{8}{5}F + \frac{16}{35}F^2)$

b. $\langle p_2\rangle = 3\,p_F\sigma_0\,(1 - \frac{14}{9}F + \frac{23}{45}F^2)/4\,\langle\sigma\rangle$

c. $\langle\cos\omega\rangle = p_F\sigma_0\,(1 - \frac{6}{5}F + \frac{1}{120}F^2)/4\,p_1\,\langle\sigma\rangle$

d. $\langle p_2\cos\omega\rangle_{\cos\omega>0} = 3\,p_F\sigma_0(1 + \frac{8}{15}F^{1/2} - \frac{7}{6}F - \frac{64}{105}F^{3/2} - \frac{5}{48}F^2)/16\,\langle\sigma\rangle$

e. $\langle p_2\cos\omega\rangle_{\cos\omega<0} = -3\,p_F\sigma_0(1 - \frac{8}{15}F^{1/2} - \frac{7}{6}F + \frac{64}{105}F^{3/2} - \frac{5}{48}F^2)/16\,\langle\sigma\rangle$

f. $\langle p_2\cos\omega\rangle = \langle p_2\cos\omega\rangle_{\cos\omega>0} + \langle p_2\cos\omega\rangle_{\cos\omega<0}$

g. $\langle p_2\sin\omega\rangle = 3\pi\,p_F\sigma_0\,(1 - \frac{7}{4}F + \frac{299}{384}F^2)/16\,\langle\sigma\rangle$

Table IV

Relativistic expressions of $\langle\sigma\rangle$ and other quantities for isotropic scattering where σ is proportional to $1/E$ and for $E_1 \geqslant 2\,E_F$

a. $$\langle\sigma\rangle = \sigma_0 \left(1 - \frac{7}{5} F - \frac{\gamma_1^4 + \gamma_1^2 + 2\gamma_1 - 2}{5(\gamma_1 + 1)} F\right)$$

b. $$\langle p_2\rangle = 3\, p_F \sigma_0 \left(1 - \frac{4}{3} F - \frac{\gamma_1^4 + \gamma_1^2 + 2\gamma_1 - 2}{9\gamma_1^2(\gamma_1 + 1)} \cdot 2F\right)$$

c. $$\langle\cos\omega\rangle = p_F \sigma_0 (\gamma_1^2 + \gamma_1 - 1)$$
$$\left(1 - \frac{4}{3} F - \frac{4\gamma_1^6 + 5\gamma_1^5 - 8\gamma_1^4 + \gamma_1^3 - 4\gamma_1^2 - 6\gamma_1 + 6}{15(\gamma_1+1)(\gamma_1^2+\gamma_1-1)} \cdot 2F\right) / 4\gamma_1 p_1 \langle\sigma\rangle$$

d. $$\langle p_2 \cos\omega\rangle_{\cos\omega > 0} = 3\, p_F \sigma_0$$
$$\left(1 + \frac{8}{15} \cdot \frac{\gamma_1^2 + \gamma_1 - 1}{\gamma_1} \sqrt{\frac{2}{\gamma_1+1}}\, F^{1/2} - \frac{4}{3} F + \frac{2\gamma_1^3 - \gamma_1^2 - 2\gamma_1 + 2}{3\gamma_1^2(\gamma_1 + 1)} F\right) / 16 \langle\sigma\rangle$$

e. $$\langle p_2 \cos\omega\rangle_{\cos\omega < 0} = -3\, p_F \sigma_0$$
$$\left(1 - \frac{8}{15} \frac{\gamma_1^2 + \gamma_1 - 1}{\gamma_1} \sqrt{\frac{2}{\gamma_1+1}}\, F^{1/2} - \frac{4}{3} F + \frac{2\gamma_1^3 - \gamma_1^2 - 2\gamma_1 + 2}{3\gamma_1^2(\gamma_1+1)} F\right) / 16 \langle\sigma\rangle$$

f. $$\langle p_2 \cos\omega\rangle = \langle p_2 \cos\omega\rangle_{\cos > 0} + \langle p_2 \cos\omega\rangle_{\cos\omega < 0}$$

g. $$\langle p_2 \sin\omega\rangle = 3\pi\, p_F \sigma_0 \left(1 - \frac{4}{3} F - \frac{2\gamma_1^4 + 2\gamma_1^3 + \gamma_1^2 + 2\gamma_1 - 2}{6(\gamma_1+1)\gamma_1^2} F\right) / 16 \langle\sigma\rangle$$

C. Inelastic Collisions[10]

In this report we consider only those inelastic collisions that lead to pion production. The formation of other particles is neglected. For inelastic collisions, the resultant energy of each nucleon depends on the energy and scattering angle of each pion that is formed in addition to the variables, E_1, E_2, ω, θ', and ϕ', present in the elastic case. From the angular distributions and momenta of the pions and nucleons (discussed below under INPUT DATA) it is possible to calculate the total energy, γ'_{final}, and the momentum, p'_{final}, of each nucleon after the interaction in the center-of-mass system. The value of E_{final} for each nucleon is given by

$$E_{final} = \frac{(\gamma_1+\gamma_2)\gamma'_{final}}{\sqrt{2(A+1)}} - 1 + \left[\frac{p_1^2+p_2^2+2p_1p_2\cos\omega}{2(A+1)}\right]^{1/2} p'_{final}\cos\chi', \tag{11}$$

where χ' is the angle between the direction of motion, $\overrightarrow{CD}$, of the center-of-mass and $\overrightarrow{p'_{final}}$ (see Fig. 1b). The angle χ' for the struck particle is shown in Fig. 1b.

The value of $\cos\chi'$ is given by

$$\cos\chi' = \mp(\cos\alpha'\cos\theta' - \sin\alpha'\sin\theta'\cos\phi'), \tag{12}$$

where α' is the angle between $\overrightarrow{CD}$ and the direction of motion, $\overrightarrow{AC}$, of the particle in the center-of-mass system before the collision (see Fig. 1b). The minus sign is for the incident particle; the plus sign is for the struck particle. The value of α' is given by

$$\sin\alpha' = p_1p_2\sin\omega / \left[(p_1^2 + p_2^2 + 2p_1p_2\cos\omega)(A-1)/2\right]^{1/2}. \tag{13}$$

In inelastic collisions the values of γ'_{final}, p'_{final}, θ' and ϕ' of the incident particle need not be the same as the corresponding values of the struck particle.

The value of E_{final} for the elastic case, see Eq. (1), can be obtained from Eq. (11) by setting γ'_{final} = one-half the total energy in the center-of-mass system, i.e. one-half of $\sqrt{2(A+1)}$.

The values of $\langle\sigma\rangle$, $\langle p_2\rangle$, etc. for inelastic collisions were not evaluated analytically. A machine computation was performed for this purpose.

D. Computation

The complex nature of nucleon-nucleon scattering compelled us to evaluate $\langle\sigma\rangle$ and the quantities related to the struck nucleon by means of machine computation for the actual experimental data. This complexity is especially marked for the higher bombarding energies where both nonisotropic and inelastic scattering are prominent.[11]

The values of $\langle\sigma\rangle$ for the general case [Eq. (2)] were computed for each value of E_1 by means of the Monte-Carlo method from

$$\langle\sigma\rangle = \frac{\Sigma\, \epsilon\, \beta'' d\sigma/d\Omega}{\beta_1\, \Sigma(d\sigma/d\Omega)/\sigma}. \tag{14}$$

where the sums are taken over a sequence of random-number quadruples, related to the kinematical variables by Eqs. (15) to (18). Here we have $\epsilon = 1$, if the energy of both particles after the collision is greater than E_F, or $\epsilon = 0$ otherwise. The quantities β'' and σ depend on p_2 (or E_2) and ω; $d\sigma/d\Omega$ on p_2, ω, θ'; and ϵ on p_2, ω, θ', and ϕ' [see Eqs. (1) and (11)]. The four independent variables necessary to evaluate each entry in Eq. (14) were obtained from the following relationships:

$$p_2 = \xi_1^{1/3}\, p_F \tag{15}$$

$$\cos\omega = 1 - 2\xi_2 \tag{16}$$

$$\cos\theta' = 1 - 2\xi_3 \tag{17}$$

$$\phi' = 2\pi\xi_4, \tag{18}$$

where each ξ is a random number in the interval 0 to 1, chosen by a method given by Olga Taussky and John Todd.[12] Equations (15) to (18) give the correct distribution of values for each of the variables. Each successive entry in Eq. (14) was evaluated by means of a new set of values for the four ξ's.

After each 100 entries, $\langle\sigma\rangle$ was evaluated for all the cases to that point for the given E_1. The computation was terminated when the value of $\langle\sigma\rangle$ varied by less than 0.375% for three successive sets of 100 entries. If this test was not satisfied but $\langle\sigma\rangle$ was less than 3.2mb, the computation was terminated. This exception was made to avoid excessive use of the computer for evaluating $\langle\sigma\rangle$ to a precision not justified by the scattering data. Approximately 1000 to 10,000 entries in Eq. (14) were required for each value of E_1.

Several checks were made of the reliability of the computation. The value of the quantity, $\Sigma(d\sigma/d\Omega)/\sigma$ in Eq. (14), should approach $n/4\pi$ for large values of n, the number of entries. This was found to be the case. In addition, the value of $\langle\sigma\rangle/\sigma_0$ with $d\sigma/d\Omega$ constant was calculated by the equation,

$$\langle\sigma\rangle/\sigma_0 = \Sigma\,\epsilon\,\beta''/n\beta_1, \tag{19}$$

where ϵ was obtained for the elastic case from Eq. (1). In the computation, entries in Eqs. (14) and (19) were made simultaneously from the same set of ξ values. The final value of $\langle\sigma\rangle/\sigma_0$ from Eq. (19) agreed with that from Eq. (a) of Table II within the statistical uncertainty of the calculation. Reproducibility tests, by making several independent calculations at the same value of E_1, confirmed the reliability of the results.

The value of $\langle\sigma\rangle$ for inelastic collisions can also be evaluated from Eq. (14), but with the values of ϵ, $d\sigma/d\Omega$, and σ appropriate to this type of collision.

The values of $\langle p_2 \rangle$, $\langle \cos\omega \rangle$, and the other properties of the struck nucleon in allowed collisions were calculated from the relation

$$\langle x \rangle = \frac{\Sigma x \epsilon \beta'' d\sigma/d\Omega}{\Sigma \epsilon \beta'' d\sigma/d\Omega} \tag{20}$$

simultaneously with the other determinations. We did not compute the final directions of motion of the nucleons and pions (or the energies of the latter), because these would have required an extensive elaboration of the computer program.

INPUT DATA

A large body of experimental data is available on nucleon-nucleon scattering at various energies.[11, 13] For convenience in machine computation, we have expressed the experimental data in the form of power-series functions of the energy and the cosine of the center-of-mass scattering angle. These expressions are given in reference 14. Only nuclear scattering was included. The contribution of Coulomb scattering was subtracted.

The values of n-p scattering cross sections below 10 Mev were taken from the compilation by Hughes and Schwartz.[13] The values for nuclear p-p scattering below 10 Mev were calculated with the aid of scattering theory.[15] At these lower energies, nucleons are thought to interact with the nucleus as a whole. The calculations for these energies are presented for completeness and also to help determine the role of nucleon-nucleon collisions in low-energy nuclear reactions. Nucleon-nucleon scattering data above 10 Mev were taken from a review article by Hess and from references listed there.[11] Elastic differential data for n-p collisions are given there only to 580 Mev. We, therefore, made the usual assumption that the n-p interaction consists of equal contributions of states with total isotopic spin T = 0 and T = 1.[15] The contribution of the state with T = 1, as obtained from differential p-p

scattering, was subtracted. The resulting values for T = 0 were extrapolated to higher energies with the aid of total elastic n-p and p-p cross sections from Hess.[11] The elastic n-p differential cross sections at these higher energies were taken to be the average of the T = 0 and T = 1 data, the latter from p-p scattering experiments.

The elastic differential cross sections were expressed as power series in $\cos\theta'$, the scattering angle in the center-of-mass system. The coefficients of the terms in these expressions were in turn fitted by the method of least squares to a power series of the energy, E. In order to do this conveniently, the data were divided into several energy intervals up to 6.2 Bev. These expressions, given in reference 14, agree with nearly all the experimental values within the quoted experimental errors. The values of σ_0 (elastic) calculated from these formulas are given in Tables V and VI. At energies of 1 Bev and greater, the elastic differential cross sections are given in reference 14 as a constant, which is a function of the energy, times $\cos^N\theta'$. The values of N from these expressions are given in the last column of Table VI. These values are considered to be the same for like-particle and unlike-particle collisions.

The treatment of inelastic collisions was not as satisfactory as that of elastic collisions. We were not able to reconcile all the available experimental data by simple polynomial expressions. Instead, we used Eq. (11) to derive expressions for the energy of each nucleon resulting from inelastic collisions, based on two different assumptions about the kinetics of the reaction. In the first, the momentum vectors of the pions and nucleons in the center-of-mass system were all assumed to be in the same plane and to be equal in magnitude. The angles between these vectors were taken to be equal.

In the second, the momentum of the pions in the center-of-mass system was taken to be zero.

We fitted only the values of the total inelastic cross sections and the meson multiplicities by power series in E, again by the method of least squares (see reference 14). Below 1 Bev, we considered only single-pion production; between 1 and 1.6 Bev only single-and double-pion production, and at higher energies triple-pion production as well. The same expressions were used for both p-p and n-p collisions. The production of four or more mesons was considered to be negligible below 6.2 Bev, the maximum energy considered.

We made only a rough evaluation of the angular distribution of the interaction products of inelastic collisions. For E less than $0.6\ m_0c^2$, we took $d\sigma/d\Omega$ of the pion to be proportional to $1 + 3\cos^2\theta$. For all other inelastic cases this expression was used for the nucleon differential cross section. The values of σ_0(inelastic) from these expressions are given in Table VII.

Table V

Values of σ_0, the free-particle elastic cross section, and also $1 - \langle\sigma\rangle / \sigma_0$ for elastic nucleon-nucleon collisions in nuclear matter for incident nucleon energies $\leq$ 50 Mev

E_1 (Mev)	σ_0 (mb) p-p or n-n	σ_0 (mb) n-p or p-n	$1 - \langle\sigma\rangle / \sigma_0 = K E_F/E_1$ for $E_F < E_1/2$: K_{p-p} or n-n	K_{n-p} or p-n	$1 - \langle\sigma\rangle / \sigma_0$ for $E_F > E_1/2$: E_F (Mev)	p=p or n-n	n-p or p-n
10	388.2	968.5	1.56				
20	160.4	520.2	1.59		12	0.809	
40	71.2	214.8	1.36	1.45	24.51	0.819	0.882
					28.45	0.905	0.923
50	56.4	159.7	1.36	1.39	28.45	0.755	0.862
					33.43	0.766	0.877

Table VI

Values of σ_0, the free-particle elastic cross section, and also $1-\langle\sigma\rangle/\sigma_0$ for elastic nucleon-nucleon collisions in nuclear matter for incident nucleon energies greater than 50 Mev.

E_1 (Mev)	σ_0 (mb)		$1-\langle\sigma\rangle/\sigma_0 = KE_F/E_1$ for $E_F < 35$ Mev		$1-\langle\sigma\rangle/\sigma_0$ for $E_F = 48.1$ Mev		N ($d\sigma/d\Omega \propto \cos^N\theta$ for $E_1 \geq 1$ Bev)
	p-p or n-n	n-p or p-n	K_{p-p} or K_{n-n}	K_{n-p} or K_{p-n}	p-p or n-n	n-p or p-n	
60	47.2	126.7	1.38	1.41	0.963	0.966	
70	40.9	105.4	1.37	1.40	0.874	0.879	
80	36.3	90.8	1.39	1.46	0.789	0.792	
90	32.8	80.4	1.36	1.53	0.722	0.732	
100	30.1	72.7	1.34	1.63	0.632	0.654	
125	25.3	60.0	1.15	1.82			
150	23.8	49.8	1.14	1.92	0.399	0.507	
175	23.7	46.2[a]	1.30	2.20[a]	0.353	0.465[a]	
200	23.6	40.9	1.41	2.13	0.324	0.409	
250	23.4	38.2	1.50	2.50	0.286	0.405	
300	23.2	36.0	1.52	2.76	0.247	0.375	
350	23.1	33.7	1.57				
400	23.1	32.3	1.48	3.15	0.196	0.343	
450	23.1	30.6	1.55	3.57	0.185	0.313	
500	23.3	28.7	1.83	3.55	0.187	0.297	
550	23.7	26.5	2.67	3.38	0.209	0.261	
600	25.0	25.3	3.81[b]	3.53	0.278	0.274	
700	23.4	22.6	3.89	3.83	0.267	0.269	
800	22.8	20.9	4.87	5.15	0.259	0.273	
900	22.0	19.5	5.94	6.97	0.271	0.301	
1000	19.9	17.3	4.68[c]	7.15	0.230	0.294	4
1250	21.2	14.1	9.73				6
1500	20.4	12.5	12.4	12.1	0.334	0.316	8
2000	18.0	10.1	15.7	15.4	0.327	0.321	11
2500	15.4	8.3	18.2[d]				13
3000	13.3	7.1	24.7	24.0	0.266	0.257	14.5

Table VI (continued)

E_1 (Mev)	σ_0 (mb)		$1-\langle\sigma\rangle/\sigma_0 = KE_F/E_1$ for $E_F < 35$ Mev		$1-\langle\sigma\rangle/\sigma_0$ for $E_F = 48.1$ Mev		N ($d\sigma/d\Omega \propto \alpha$ $\lvert\cos\theta\rvert^N$ for $E_1 \geq 1$ Bev)
	p-p or n-n	n-p or p-n	K_{p-p} or K_{n-n}	K_{n-p} or K_{p-n}	p-p or n-n	n-p or p-n	
4000	9.6	5.3	23.6	23.4	0.269	0.269	18
5000	8.6	5.0	43.9	46.9	0.304	0.321	24.5
6000	7.3	4.1	57.1	55.3	0.381	0.374	37

[a]Incorrect value of σ_0 given by expressions in reference 14. Values given here have been corrected to σ_0 = 46.2 mb (see text).

[b]The value of $K_{p-p, n-n}$ is 2.69 when based on σ_0 = 23.6 mb.

[c]The value of $K_{p-p, n-n}$ is 7.44 when based on σ_0 = 21.7 mb.

[d]Based on E_F = 18.8 Mev only.

Table VII

Values of σ_0 the free-particle cross section, used in the calculations here, for inelastic collisions involving one-, two-and three-pion production.

E_1 (Mev)	σ_0 (p-p or n-n) (mb)			σ_0 (p-n or n-p) (mb)		
	one pion	two pions	three pions	one pion	two pions	three pions
350	0.68			0.34		
400	1.77			0.97		
450	3.65			2.11		
500	6.0			3.55		
550	8.7			5.2		
600	11.7			6.9		
700	17.8			10.4		
800	23.4			13.5		
900	27.7			16.0		
1000	28.3	0.7		17.4	0.5	
1500	21.3	5.8		22.8	6.2	
2000	17.0	7.4	1.5	19.8	8.7	1.8
3000	12.9	8.8	4.3	13.7	9.4	4.6
4000	10.6	8.7	6.7	10.6	8.7	6.7
5000	9.2	8.2	8.6	9.2	8.2	8.6
6000	8.1	7.7	10.2	8.1	7.7	10.2

RESULTS

In this section we present the results of the machine computation of $\langle\sigma\rangle_{elastic}$ and $\langle\sigma\rangle_{inelastic}$ by Eq. (14) and the quantities, $\langle p_2\rangle$, $\langle\cos\omega\rangle$, etc., by Eq. (20) for collisions between like particles, p-p and n-n, and between unlike particles, p-n and n-p, as a function of the energy of the incident particle. For convenience, we designate the like-particle case by "p-p or n-n" and the unlike-particle case by "n-p or p-n". We compare these results with the expressions of Tables I to IV.

A. $\langle\sigma\rangle_{elastic}$

The values of $\langle\sigma\rangle$ for the elastic case were evaluated by means of Eq. (14). To show the effect of exclusion clearly, we have expressed the results of the calculation as $1-\langle\sigma\rangle/\sigma_0$. This is also helpful in comparing the computed results with the equations given in Tables I to IV.

We were able to improve the accuracy of these values, without further use of the computer, by means of the following expression.

$$1 - \langle\sigma\rangle/\sigma_0 = C(1 - \langle\sigma\rangle/\sigma_0)_{Eq.(14)}, \tag{21}$$

where $(1 - \langle\sigma\rangle/\sigma_0)_{Eq.(14)}$ is the value computed by means of Eq. (14), and C is the ratio of $(1 - \langle\sigma\rangle/\sigma_0)$ calculated by means of Eq. (a) of Table II and that computed from Eq. (19). Any deviation in $1 - \langle\sigma\rangle/\sigma_0$ by use of Eq. (19) from that by Eq. (a) of Table II will be reflected in a similar deviation in the value calculated using Eq. (14). Hence, we expect the factor C will provide a correction for the statistical error of the computation. The value of C should approach unity as the number of entries in Eq. (19) increases. This was found to be the case.

The results for elastic collisions with different values of E_F were fitted to the equation

$$1 - \langle\sigma\rangle/\sigma_0 = K\,E_F/E_1 = KF \qquad (22)$$

by the method of least squares with a deviation of several percent or less. Here K is a constant at each value of E_1, the incident energy, for $E_F \lesssim E_1/2$. This type of fit is suggested by Eqs. (a) of Table I and II. The values of K obtained from the data given by Eq.(14) agree with those given by Eq.(21) with an average deviation of approximately 1%. However, the fit to Eq.(22) was better for the values of $\langle\sigma\rangle/\sigma_0$ calculated by means of Eq.(21).

The values of K based on Eq.(21) are given in Table V for incident energies of 50 Mev and less and in Table VI for 60 Mev and greater. The values for collision between like particles are listed under $K_{p\text{-}p \text{ or } n\text{-}n}$ and for collisions between unlike particles under $K_{n\text{-}p \text{ or } p\text{-}n}$. These values are plotted in Fig. 2. The values of K given in Table V were obtained with several values of $E_F \lesssim E_1/2$. The results for greater values of E_F are given in the last two columns as $1 - \langle\sigma\rangle/\sigma_0$.

The results given in Table VI were calculated for E_F = 18.8, 24.5, 28.5, 33.4, and 48.1 Mev except in those cases for which no value of $K_{n\text{-}p \text{ or } p\text{-}n}$ is listed. In the latter cases the neutron and proton were assigned different Fermi energies. The fit to Eq.(22) is best for E_F in the range 18.8 to 33.4 Mev. The values of K for these cases are given in Table VI. The values of $1 - \langle\sigma\rangle/\sigma_0$ at E_F = 48.1 Mev, calculated according to Eq.(14) are also listed in Table VI. The latter values were essentially identical with those obtained from Eq.(21) at nearly all energies. In the second and third columns of Tables V and VI are given the values of σ_0, calculated by the formulas of reference 14, unless indicated otherwise. These agree very well with the experimental values except for the unlike-particle case at 175 Mev.

The values of $1 - \langle\sigma\rangle/\sigma_0$, and hence K, are sensitive to the value of σ_0. The value of $\langle\sigma\rangle$ itself, on the other hand, is relatively insensitive to σ_0 because very few collisions have the same center-of-mass energy as that for the struck particle at rest. The values of $1 - \langle\sigma\rangle/\sigma_0$ (and K) at any incident energy can be corrected for a different value of σ_0 from that given in Tables V and VI, providing the adjacent values of σ_0 in these tables and the corresponding angular distributions are unchanged. We have made such corrections with new values of σ_0 for like-particle collisions at 600 Mev, 23.6 mb, and at 1.0 Bev, 21.7 mb, which we obtained by interpolation of adjacent values. We determined a corrected value of $\langle\sigma\rangle/\sigma_0$ at $E_F = 26.3$ Mev, the average of the four values of E_F used to determine K. By this means we obtained the new values, $K_{p\text{-}p \text{ or } n\text{-}n} = 2.69$ at 600 Mev, and 7.44 at 1.0 Bev. This procedure, while not as correct as repeating the machine computation with the new value of σ_0, is probably justified by the uncertainties in the experimental measurement of σ_0.

For all the entries in Tables V and VI, the Fermi energies of the incident and struck particles are equal. In general, however, the neutron and proton Fermi energies are different for any given nucleus. Tables V and VI are, of course, still valid for collisions between like particles. In the case of collisions between unlike particles we have found the following relations to fit the data very well:

Neutron Fermi energy is larger than proton Fermi energy, or $F_n > F_p$

(a) Incident particle is a neutron

$$1 - \langle\sigma\rangle/\sigma_0 = K_{n\text{-}p \text{ or } p\text{-}n}(0.7F_n + 0.3F_p) \tag{23}$$

(b) Incidnet particle is a proton

$$1 - \langle\sigma\rangle/\sigma_0 = K_{n\text{-}p \text{ or } p\text{-}n}(0.5F_n + 0.5F_p) \tag{24}$$

Proton Fermi energy is larger than neutron Fermi energy, or $F_p > F_n$

(a) Incident particle is a proton

$$1 - \langle \sigma \rangle / \sigma_0 = K_{n-p \text{ or } p-n}(0.7 F_p + 0.3 F_n) \tag{25}$$

(b) Incident particle is a neutron

$$1 - \langle \sigma \rangle / \sigma_0 = K_{n-p \text{ or } p-n}(0.5 F_p + 0.5 F_n) \tag{26}$$

The values of $K_{n-p \text{ or } p-n}$ are taken from Tables V and VI. These relations were obtained with various values of F_n and F_p and agree closely with Eq. (19). A number of cases were computed with the Fermi energy of one particle set equal to zero. These cases also agreed with Eqs. (23) to (26).

B. $\langle \sigma \rangle_{\text{inelastic}}$

The values of $\langle \sigma \rangle$ for inelastic collisions were evaluated separately for the cases involving the production of one, two and three pions by means of Eq. (14). The values of E_F used here were the same as those given above for the elastic case.

The resulting values of $\langle \sigma \rangle$ for like-particle collisions, based on the assumption that the center-of-mass momenta of the pions and nucleons are all equal, are shown in Figs. 3 to 5. These values are not very different from those based on the other assumption about the pion momentum--that it is zero in the center-of-mass system--as can be seen from Table VIII. The ratios given in Table VIII are the same for the like-and the unlike-particle cases at the same value of E_F. Each value given in Table VIII is the average for the five different Fermi energies. The value following the ± sign is the average deviation of the individual values from this mean value and results from the variation of the ratio with the Fermi energy. For single-pion production the ratio increases with increasing Fermi energy. For two-and three-pion production the ratio decreases

as E_F increases. With this information and the values given in Table VIII we can obtain the ratio at each of the five values of E_F. The ratios for other values of E_1 can be obtained by interpolation. The values estimated in this way agree to within 1 or 2% with the values computed directly.

The value of $\langle\sigma\rangle$ for unlike-particle collisions can be obtained by multiplying the values for the like-particle collisions given in Figs. 3 to 5 by the ratio of the two cross sections, given in Table IX. These values of $\langle\sigma\rangle_{n\text{-}p \text{ or } p\text{-}n}/\langle\sigma\rangle_{p\text{-}p \text{ or } n\text{-}n}$ are identical for the two assumptions about the pion momentum in the center-of-mass system. The values following the ± sign are average deviations from the mean and indicate the magnitude of the trend of the ratios with E_F. For $E_1 \leqslant 1000$ Mev, the ratio increases as E_F increases for all three cases of pion production. At 1500 and 2000 Mev, the variation is in the opposite direction.

C. $\langle p_2\rangle$, $\langle\cos\omega\rangle$, $\langle p_2 \cos\omega\rangle_{\cos\omega>0}$, $\langle p_2 \cos\omega\rangle_{\cos\omega<0}$, and $\langle p_2 \sin\omega\rangle$

The values of $\langle p_2\rangle$, $\langle\cos\omega\rangle$, $\langle p_2 \cos\omega\rangle_{\cos\omega\geqslant 0}$, $\langle p_2 \cos\omega\rangle_{\cos\omega<0}$, and $\langle p_2 \sin\omega\rangle$ were evaluated by means of Eq. (20) for elastic and inelastic collisions. We consider the elastic case first.

The values of $\langle p_2\rangle/p_F$ obtained in this manner are plotted in Fig. 6 as a function of E_F/E_1 (or F) for both the like-particle and the unlike-particle cases. The curve shown in Fig. 6 was calculated by using Eq. (b) of Table I for $F < 1/2$ and an equivalent expression for $F > 1/2$. The values from Eq. (b) of Table III are the same as those from Eq. (b) of Table I within a fraction of a percent. The agreement between the points and the curve is close. The computed values of $\langle p_2\rangle/p_F$ (elastic) are displayed in Figs. 7 and 8 as a function of E_1 for $E_F = 18.8$ Mev and for $E_F = 33.4$ Mev.

Tabel VIII

The ratio of $\langle \sigma \rangle$ (inelastic) for p_π (c.m.) = 0 to $\langle \sigma \rangle$ (inelastic) for p_π (c.m.) = $p_{nucleon}$ (c.m.) for one-, two-, and three- pion production.

One pion[a]		Two or three pions[b]	
E_1 (Mev)	Ratio	E_1 (Mev)	Ratio
400	0.91 ± 0.04[c]	900	0.86 ± 0.03[d]
700	0.93 ± 0.02	1000	0.89 ± 0.04[d]
1000	0.95 ± 0.01	2000	0.96 ± 0.02
$\geqslant$4000	0.99 ± 0	$\geqslant$4000	0.98 ± 0.01

[a]Ratio increases with increasing E_F.

[b]Ratio decreases with increasing E_F.

[c]These values are for 18.8 Mev $\leqslant E_F \leqslant$ 33.4 Mev Ratio, at E_F = 48.1 Mev, = 1.16

[d]Only for two-pion production. $\sigma(3\pi$ production) = 0.

Table IX

$\langle\sigma\rangle_{\text{n-p or p-n}} / \langle\sigma\rangle_{\text{p-p or n-n}}$ for inelastic collisions involving one-, two-, and three-pion production.

E_1 (Mev)	One pion	Two or three pions
200	0.44 ± 0.06	
250	0.51 ± 0.02	
300	0.55 ± 0.01	
350 to 700	0.58 ± 0	0.56 ± 0.03[a,b]
800	0.60 ± 0.01	0.64 ± 0.02[b]
900	0.62 ± 0.01	0.69 ± 0.02[b]
1000	0.65 ± 0.01	0.75 ± 0.03[b]
1500[c]	0.97 ± 0.01	1.05 ± 0[d] 1.17 ± 0[e]
2000[c]	1.14 ± 0.01	1.15 ± 0.01
3000	1.06 ± 0	1.05 ± 0
≥4000	1.00 ± 0	1.00 ± 0

[a]Double-meson production begins at 600 Mev for $E_F \geq 33.4$ Mev. (see Fig. 4).

[b]Only for two-pion production, σ (3π production) = 0.

[c]Ratio decreases with increasing E_F. Ratio is constant or increases with increasing E_F for all other cases.

[d]For two-pion production.

[e]For three-pion production.

The computed values of $\langle \cos\omega \rangle$ and those of the average of various projections of the momenta of the struck particle are also shown in Figs. 7 and 8. The computed values agree closely with the curves calculated by using the appropriate equations given in Tables I to IV. The agreement is best for $\langle p_2 \rangle$ and for $\langle p_2 \sin\omega \rangle$. Thus, for $E_1 < 200$ Mev the equations in Tables III and IV fit the computed values quite well. Here, the experimentally determined cross sections are isotropic and vary inversely with energy, and the agreement is good. At higher energies the equations in Tables I and II fit the like-particle results better. Here, the cross sections are nearly constant. This is not the case for collisions between unlike particles. For such collisions a clear-cut comparison cannot be made because the angular distributions are not isotropic. Above approximately 500 Mev the like-particle collisions become increasingly nonisotropic. However, at these energies both types of relativistic formulations in Tables II and IV converge to the values that one would expect without the imposition of the exclusion principle. The two formulations appear to be equally good (or bad).

A similar set of comparisons is made in Figs. 6, 9, 10, and 11 for the inelastic case. Here too, the equations in Tables II and IV give values that agree with the computed results in the multi-Bev region of bombarding energies. At energies closer to the thresholds for single- and for multiple-pion production, strong deviations occur. These deviations are to be expected, of course. Large values of p_2 and ω are favored, for these result in the largest center-of-mass energies (see Fig. 1) and hence the largest cross sections. This is due to the sharp rise in the inelastic cross section with energy above the threshold. In Figs. 6, 9, 10, and 11 a large increase in the value of $\langle p_2 \rangle / p_F$ occurs as the energy of the incident particle decreases. The other quantities, in contrast, decrease rapidly in value as E_1 decreases. Here we see the tendency toward large collision angles.

SUMMARY

The effect of the exclusion principle on the elastic cross section is large even at high incident energies, as can be seen in Tables V and VI. This is due to the strong forward scattering at these energies, which counterbalances the effect of the decreasing values of E_F/E_1. The values of $\langle\sigma\rangle_{\text{inelastic}}$ show the effects of both the exclusion principle and the rapid rise of the free-particle inelastic cross section near the threshold. The effect of the latter is pronounced at lower energies, resulting in an increase in $\langle\sigma\rangle_{\text{inelastic}}$ as E_F increase (see Figs. 3 to 5). At intermediate energies, the effect of exclusion causes a small drop in $\langle\sigma\rangle_{\text{inelastic}}$ for single- and double-pion production (Figs. 3 and 4). The effect is more noticeable for single-pion production. At the highest energies the inelastic cross sections are essentially unaffected by the exclusion principle. It is our hope that the values of $\langle\sigma\rangle$ given here will be useful in the interpretation of nuclear cross-section measurements.

The values of $\langle p_2\rangle$, $\langle\cos\omega\rangle$, and the other quantities in elastic collisions can be determined either by machine computation or from the equations given in Tables I to IV. Agreement between the two methods, while not complete, is probably adequate for many purposes. The values for inelastic collisions near the threshold for pion production deviate strongly from those given by the analytical expressions. This is not surprising since the latter were obtained for elastic collisions. As the bombarding energy increases, the values of these quantities for both elastic and inelastic collisions converge to the original values of these quantities before the collision.

One possible application of these results is in the interpretation of recoil experiments.[16] Some high-energy reactions involve the ejection of a single particle. An example of this type is the (p, pn) reaction, such as

$Cu^{65}(p, pn)\ Cu^{64}$. If both the incident and the struck particles leave the nucleus without further interaction, the nucleus left behind (Cu^{64} in the example given here) will recoil with a momentum which depends on that of the ejected nucleon. The momentum of the recoiling nucleus can be measured. Comparisons of this type with the values of $\langle p_2 \rangle$, $\langle p_2 \sin\omega \rangle$, and $\langle p_2 \cos\omega \rangle$, given here may provide an effective probe of the momentum distribution of the nuclear particles.

ACKNOWLEDGMENT

We wish to thank Professor A. L. Turkevich for helpful advice.

This work was done under the auspices of the U. S. Atomic Energy Commission.

REFERENCES

1. N. Metropolis, R. Bivins, M. Storm, A. Turkevich, J. M. Miller, and G. Friedlander, Phys. Rev. 110, 185, 204 (1958). Further references are given here.
2. D. R. Nethaway and L. Winsberg, Phys. Rev. 119, 1375 (1960). Interaction of High-Energy Protons with Indium, Lawrence Radiation Laboratory Report UCRL-8908, December 1959 (unpublished). Further references are given here.
3. M. L. Goldberger, Phys. Rev. 74, 1269 (1948).
4. Y. Yamaguchi, Progr. Theoret. Phys. (Kyoto) 5, 332 (1950).
5. S. Hayakawa, M. Kawai, and K. Kikuchi, Progr. Theoret. Phys. (Kyoto) 13, 415 (1955).
6. E. Clemental and C. Villi, Nuovo cimento 2, 176 (1955).
7. I. G. Ivanter and L. B. Okun, J. Exptl. Theoret. Phys. (USSR) 32, 402 (1957); [translation: Soviet Phys. JETP 5, 340 (1957)].
8. R. M. Sternheimer, Phys. Rev. 106, 1027 (1957).
9. J. R. Fulco, Phys. Rev. 114, 374 (1959).
10. R. L. Bivins, N. Metropolis, and A. L. Turkevich, Coordinate Transformations in Intranuclear Cascade Studies, Los Alamos Scientific Laboratory Report LAMS-2360, February 1960 (unpublished).
11. W. N. Hess, Revs. Modern Phys. 20, 368 (1958).
12. Olga Taussky and John Todd in Symposium on Monte Carlo Methods, 1954, Herbert A. Meyer, Editor (John Wiley and Sons, New York, N. Y. 1956), p. 18.
13. D. J. Hughes and R. B. Schwartz, Neutron Cross Sections, BNL-325, July 1958 (unpublished).

14. T. P. Clements and L. Winsberg, Polynomial Fits of Nucleon-Nucleon Scattering Data, UCRL-9043, February 1960 (unpublished).

15. H. A. Bethe and P. Morrison, Elementary Nuclear Theory (John Wiley and Sons, New York, 1956).

16. L. Winsberg, The Mathematical Treatment of Data from Recoil Experiments, UCRL-8618, January 1959 (unpublished), p. 44.

FIGURE LEGENDS

Fig. 1. Kinematics of nucleon-nucleon collisions in the (a) laboratory system and (b) center-of-mass system.

Fig. 2. The variation of K in the expression $\langle\sigma\rangle = \sigma_0 (1-KE_F/E_1)$ for elastic nucleon-nucleon collisions as a function of the energy, E_1, of the incident nucleon. Like-particle collisions are indicated by p-p or n-n, unlike-particle collisions by n-p or p-n. See Tables V and VI.

Fig. 3. The values of $\langle\sigma\rangle$ in inelastic nucleon-nucleon collisions for single-pion production based on the assumption that the center-of-mass momenta of the pion and the nucleons are equal.

Fig. 4. The values of $\langle\sigma\rangle$ in inelastic nucleon-nucleon collisions for double-pion production based on the assumption that the center-of-mass momenta of the pions and the nucleons are equal.

Fig. 5. The values of $\langle\sigma\rangle$ in inelastic nucleon-nucleon collisions for triple-pion production based on the assumption that the center-of-mass momenta of the pions and the nucleons are equal.

Fig. 6. The values of $\langle p_2\rangle / p_F$ as a function of E_F/E_1. Computed values for elastic collisions are indicated by the symbols:

Collision type	E_1 (Mev) 0 - 50	60 - 100	125 - 450	> 450
p-p or n-n	○	△	□	•
n-p or p-n	●	▲	■	•

Values calculated by using Eqs. (b) of Tables I and III for $E_F/E_1 \leq 0.5$ are indicated by the solid line. Computed values for inelastic collisions leading to single-pion production are indicated by the broken lines.

Fig. 7. Average values of quantities related to the struck nucleons in elastic collisions for E_F = 18.8 Mev. The momentum of the struck particle is p_2, the Fermi momentum is p_F, and the collision angle is ω. Computed values are indicated by open symbols for like-nucleon collisions and by closed symbols for collisions between unlike nucleons. Values calculated by using the equations in Tables I to IV are indicated by solid lines for σ_0 = constant and by dashed lines for $\sigma_0 \sim 1/E$. The solid and dashed lines coincide for $\langle p_2 \rangle / p_F$.

Fig. 8. Average values of quantities related to the struck nucleons in elastic collisions for E_F = 33.4 Mev. For notation, see Fig. 7.

Fig. 9. Average values of quantities related to the struck nucleons in inelastic collisions resulting in single-pion production for E_F = 18.8 Mev and 33.4 Mev. For notation, see Fig. 7. The values given by the equations in Tables I to IV for F = 0 are indicated by the horizontal lines. (The value for $\langle \cos \omega \rangle$ is 0 since p_F = 0 when F = 0.)

Fig. 10. Average values of quantities related to the struck nucleons in inelastic collisions resulting in double-pion production for E_F = 18.8 Mev and 33.4 Mev. For notation, see Fig. 7. For explanation of horizontal lines, see Fig. 9.

Fig. 11. Average values of quantities related to the struck nucleons in inelastic collisions resulting in triple-pion production for E_F = 18.8 Mev and 33.4 Mev. For notation, see Fig. 7. For explanation of horizontal lines, see Fig. 9.

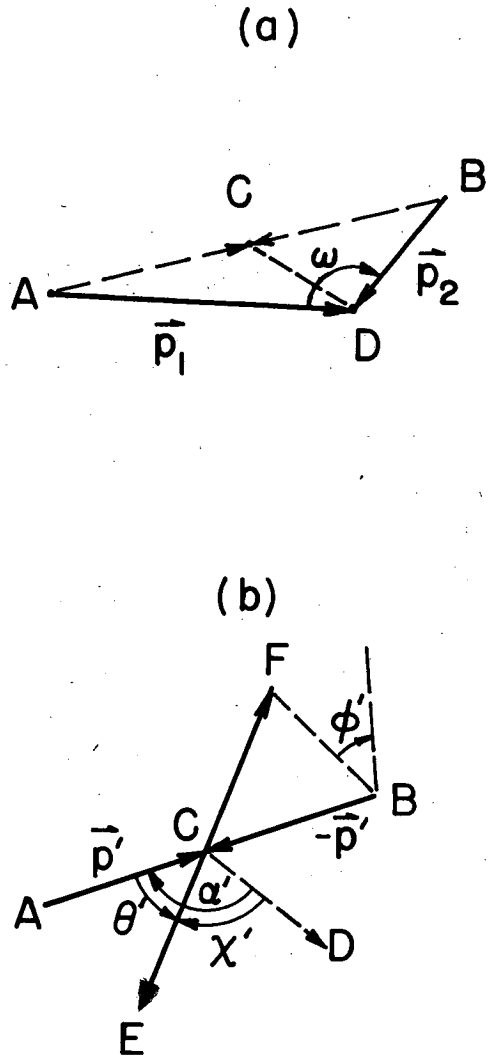

MU-21167

Fig. 1

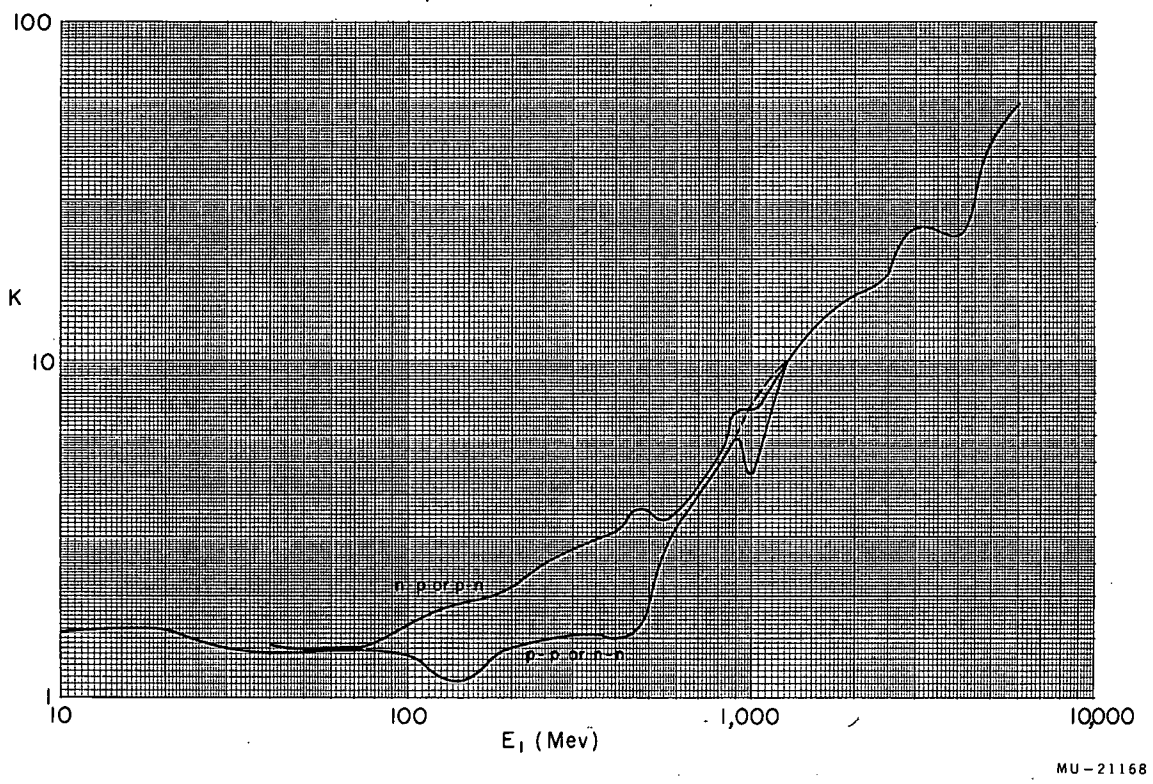

Fig. 2

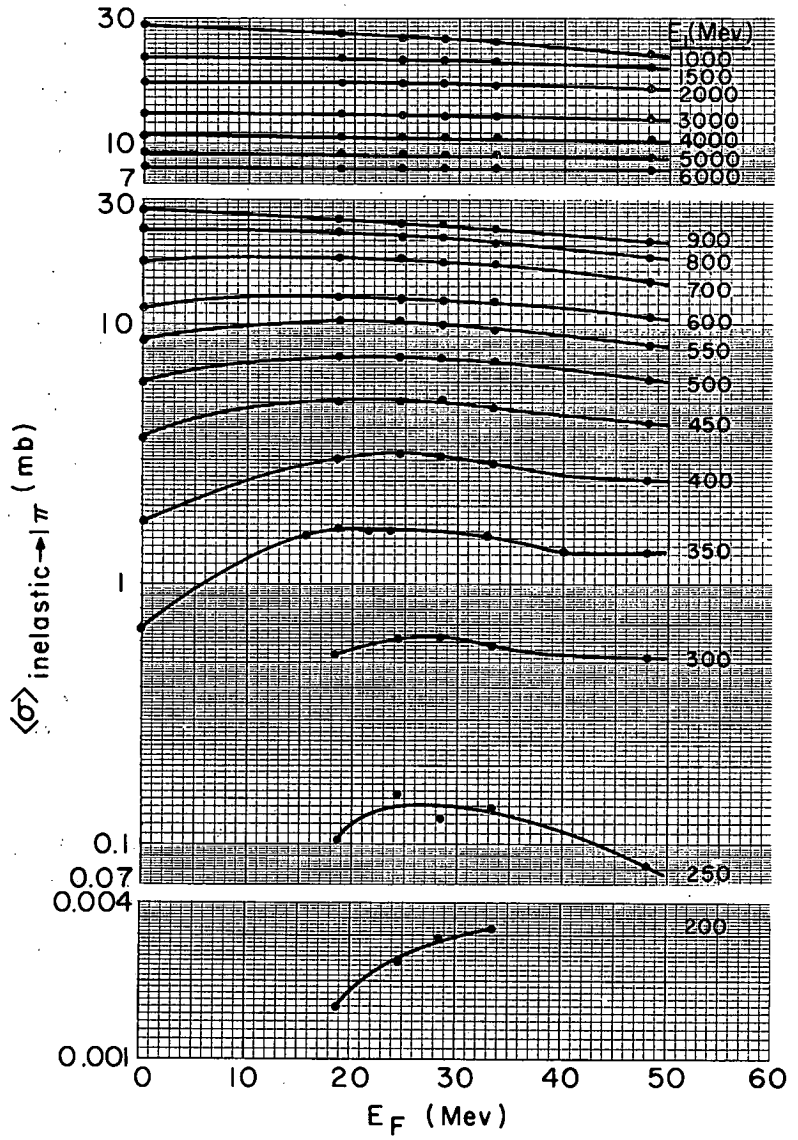
E_π (Mev)
1000
1500
2000
3000
4000
5000
6000
900
800
700
600
550
500
450
400
350
300
250
200
30
10
7
1
0.1
0.07
0.004
0.001
$\langle\sigma\rangle_{inelastic\to\pi}$ (mb)
0
10
20
30
40
50
60
E_F (Mev)
MU-21169

Fig. 3

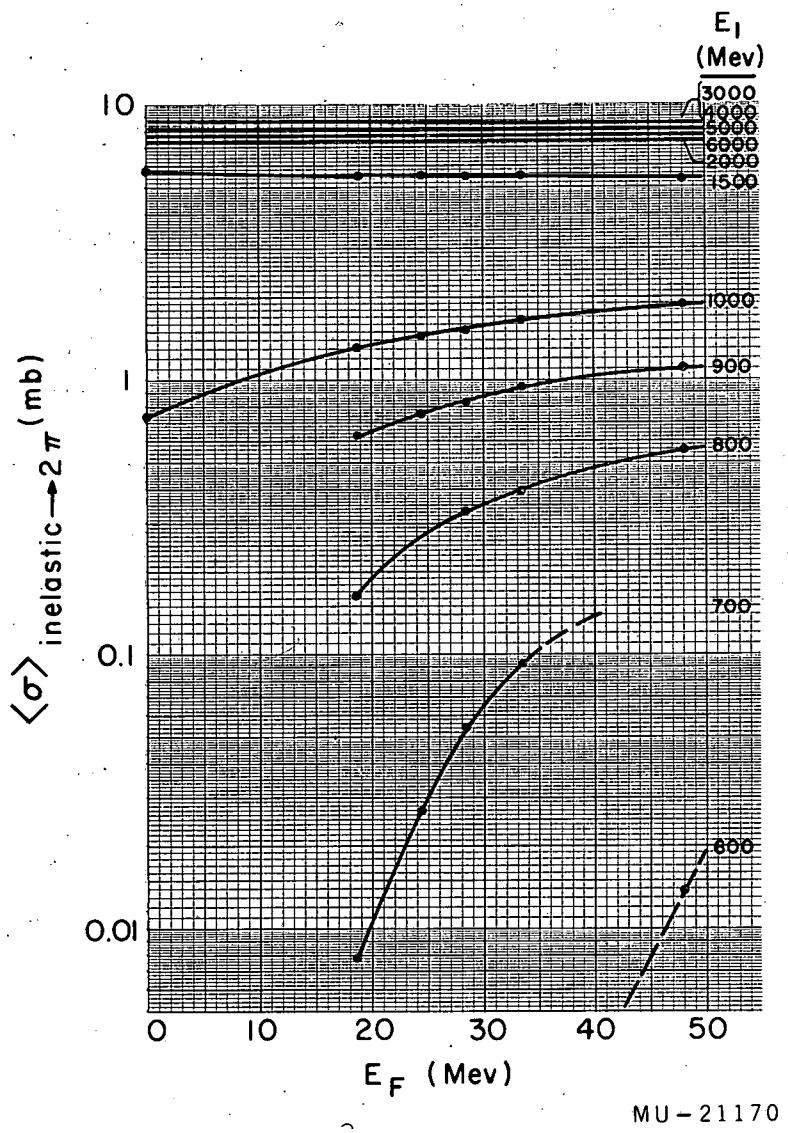
E_I (Mev)
3000
4000
5000
6000
2000
1500
1000
900
800
700
600
10
1
0.1
0.01
$\langle\sigma\rangle_{inelastic \rightarrow 2\pi}$ (mb)
0
10
20
30
40
50
E_F (Mev)
MU-21170

Fig. 4

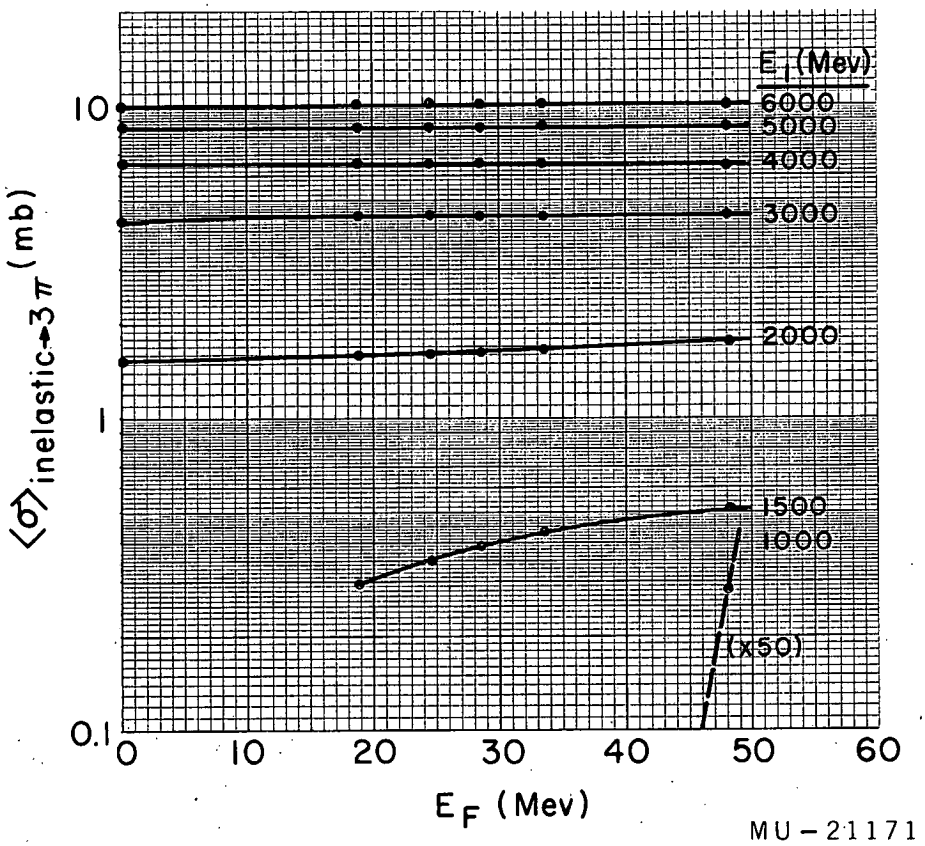
E_i (Mev)
6000
5000
4000
3000
2000
1500
1000
(x50)
10
1
0.1
0
10
20
30
40
50
60
$\langle\sigma\rangle_{inelastic \to 3\pi}$ (mb)
E_F (Mev)
MU-21171

Fig. 5

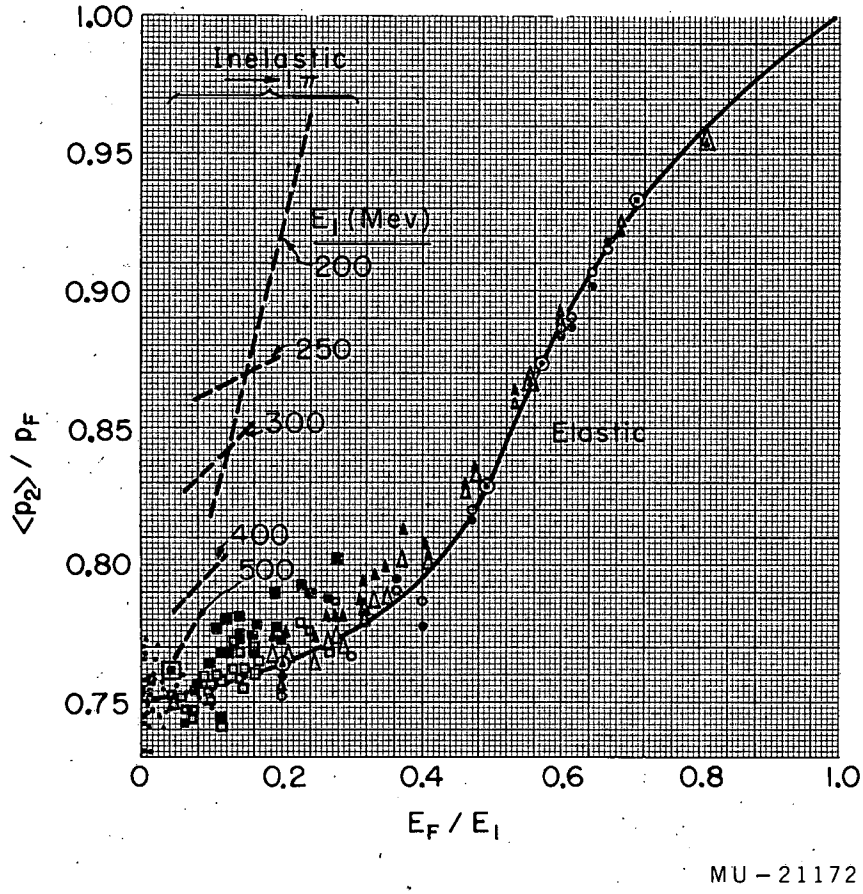
1.00
0.95
0.90
0.85
0.80
0.75
0
0.2
0.4
0.6
0.8
1.0
Inelastic
E_I (Mev)
200
250
300
400
500
Elastic
$\langle p_2 \rangle / p_F$
E_F / E_I
MU-21172

Fig. 6

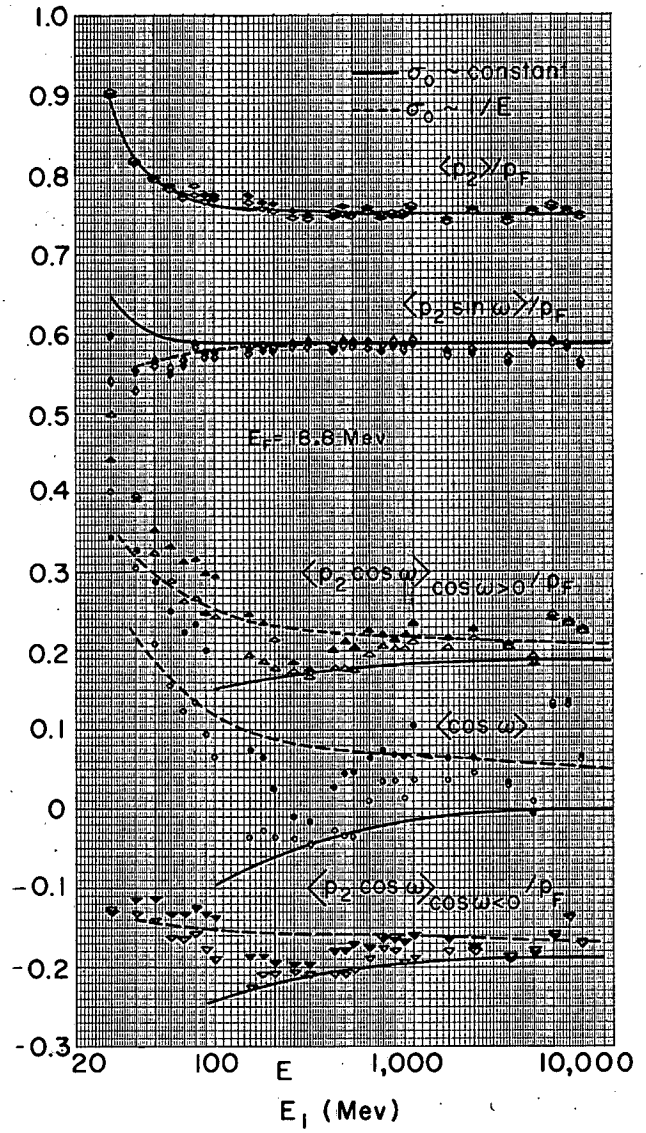
1.0
0.9
0.8
0.7
0.6
0.5
0.4
0.3
0.2
0.1
0
-0.1
-0.2
-0.3
20
100
1,000
10,000
E
E1 (Mev)
σ0 ~ constant
σ0 ~ /E
⟨p2⟩/pF
⟨p2 sin ω⟩/pF
EF = 8.6 Mev
⟨p2 cos ω⟩cos ω>0/pF
⟨cos ω⟩
⟨p2 cos ω⟩cos ω<0/pF
MU-21173

Fig. 7

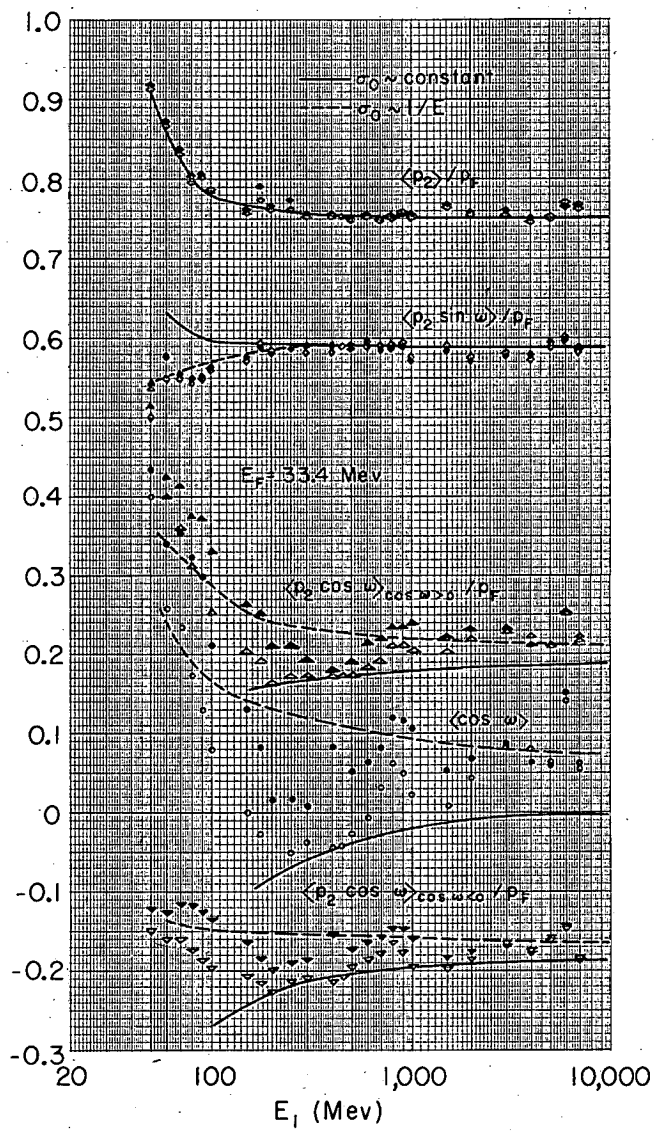

MU-21174

Fig. 8

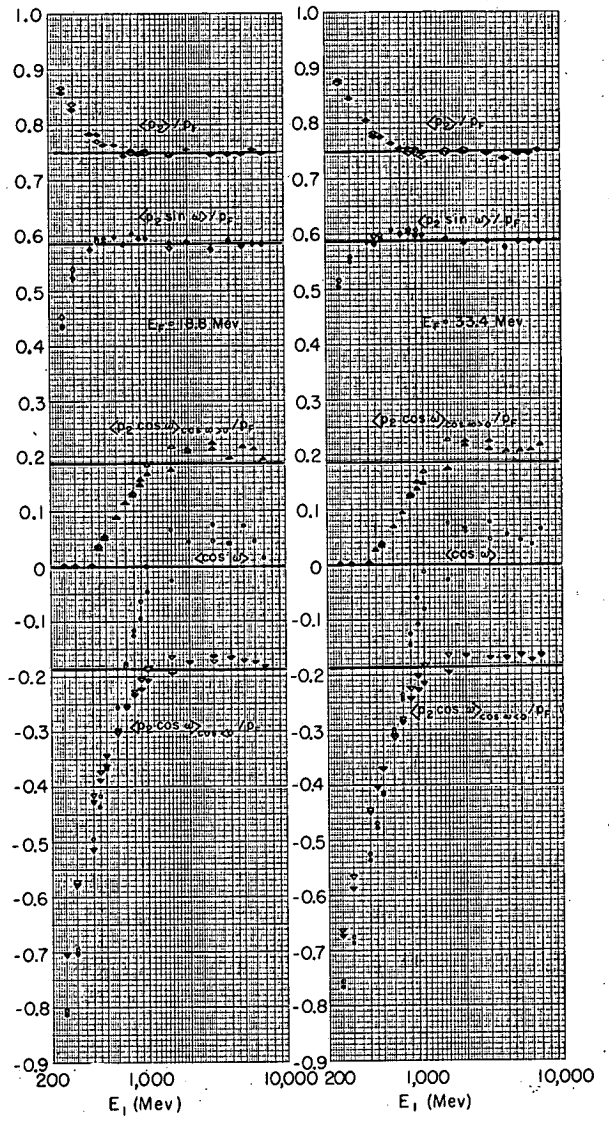
1.0
0.9
0.8
0.7
0.6
0.5
0.4
0.3
0.2
0.1
0
-0.1
-0.2
-0.3
-0.4
-0.5
-0.6
-0.7
-0.8
-0.9
200
1,000
10,000
E1 (Mev)
E1 (Mev)
MU-21175

Fig. 9

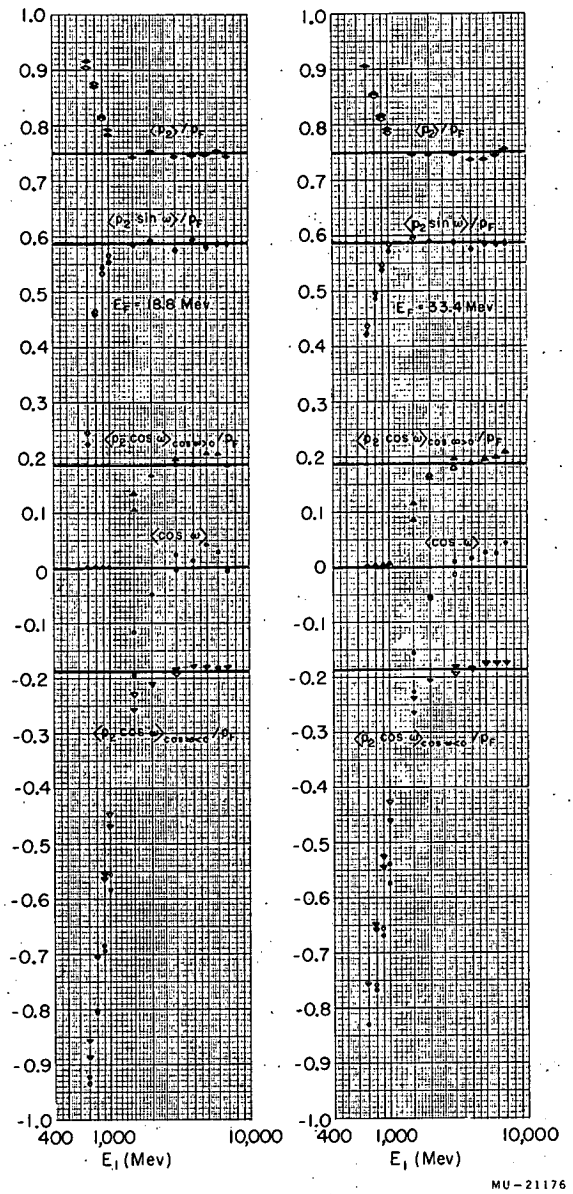
1.0
0.9
0.8
0.7
0.6
0.5
0.4
0.3
0.2
0.1
0
-0.1
-0.2
-0.3
-0.4
-0.5
-0.6
-0.7
-0.8
-0.9
-1.0
400
1,000
10,000
E1 (Mev)
E_F = 18.6 Mev
E_F = 53.4 Mev
MU-21176

Fig. 10

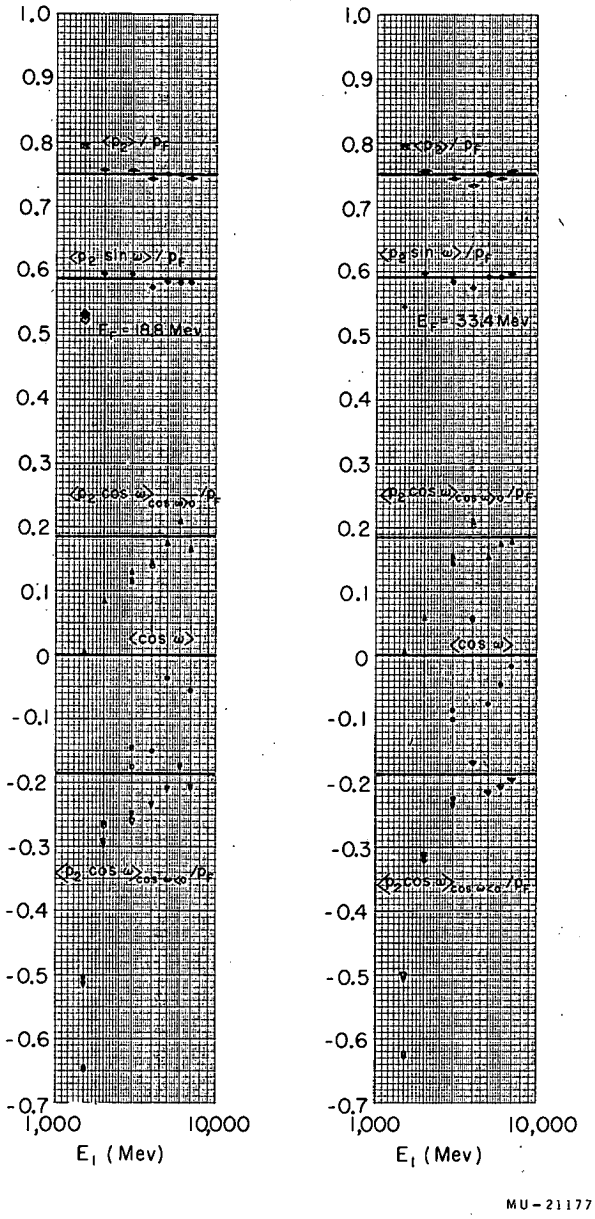
1.0
0.9
0.8
0.7
0.6
0.5
0.4
0.3
0.2
0.1
0
-0.1
-0.2
-0.3
-0.4
-0.5
-0.6
-0.7
1,000
10,000
E_I (Mev)
E_F = 18.8 Mev
E_F = 33.4 Mev
MU-21177

Fig. 11

This report was prepared as an account of Government sponsored work. Neither the United States, nor the Commission, nor any person acting on behalf of the Commission:

A. Makes any warranty or representation, expressed or implied, with respect to the accuracy, completeness, or usefulness of the information contained in this report, or that the use of any information, apparatus, method, or process disclosed in this report may not infringe privately owned rights; or

B. Assumes any liabilities with respect to the use of, or for damages resulting from the use of any information, apparatus, method, or process disclosed in this report.

As used in the above, "person acting on behalf of the Commission" includes any employee or contractor of the Commission, or employee of such contractor, to the extent that such employee or contractor of the Commission, or employee of such contractor prepares, disseminates, or provides access to, any information pursuant to his employment or contract with the Commission, or his employment with such contractor.